The Synthesis and Evaluation of a More Highly Conjugated Molecular Transporter

By

Aaron M. Almeida

****

Submitted in partial fulfillment
of the requirements for
Honors in the Department of Chemistry

UNION COLLEGE
June, 2007

Table of Contents

Figures

Abstract

Molecular transporters are a class of compounds displaying high efficiency for traversing the cellular membrane. Multiple naturally occurring proteins are efficient at crossing the cell membrane and further studies indicated the important regions for inducing cellular uptake are highly cationic, containing multiple arginine amino acids. The guanidinium head group of the arginine side chain appears to be the primary factor in determining uptake efficiency, however the method of internalization is currently unknown. One uptake theory suggests passive diffusion through the formation of less-polar complexes at the membrane surface is responsible for uptake, though the molecular details remain unclear. We aim to elucidate the role of polarizability in cell penetration. We report the design and synthesis of a peptoid molecular transporter with the highly conjugated, polarizable guanine as the pendant side chain. The transporter was synthesized by attachment of a guanine precursor to a nonamer peptoid chain. The side chain precursor, 2-chloroethylguanine, was synthesized in an overall yield of 52 % without chromatography or steric blocking groups. Selective crystallization yielded the desired N9 regioisomer, eliminating the need for preparative chromatography. Comparative cellular assays with fluorescently tagged peptoids were carried out to measure the efficiency of internalization.

Introduction

Cellular Membrane:

Biological membranes evolved over time to prevent the entrance of xenobiotics into the cell.[1] The cell membrane still has to remain permeable to beneficial components however, and so numerous systems for entry into the cell have evolved. Transporters, translocases, permeases, pores, channels, and pumps are a few examples of cellular entry mechanisms involved in allowing desired compounds through the cell membrane.[2] While enormously important for the survival of the cell, the cell membrane's selectivity for entrance into the cell limits the development of therapeutics with internal cellular targets. There is substantial interest in the development of methods for facilitating the delivery of molecules into mammalian cells. [3,4,5]

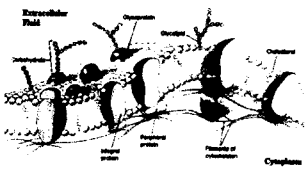

Figure 1. Cartoon of Cell Membrane

Drug Design Limitations:

The presence of the nonpolar lipid layer separating the environment from the aqueous internal cavity creates a structural limitation on nascent therapeutics with intracellular targets. Only a very narrow range of hydrophobicities can be used, as drugs must be polar enough to enter the blood, enabling them to travel to the membrane of their target cells, and non-polar enough for diffusion through the cell membrane. Also the molecules must be small enough to diffuse through the cell

membrane, as size indirectly relates to the ability of the molecule to diffuse through the membrane. Structurally speaking limits molecules to less than five hydrogen bonding donor sites, less than 10 hydrogen bond acceptor sites, and a mass less than five hundred a.m.u.,

Protein Study Limitations:

Another membrane induced limitation is the *in vivo* study of proteins. Options for delivering functional proteins into cells are limited and often have high toxicity rates due to membrane disruption. While there are methods for introducing transcriptionally active DNA into cells, the method is extremely difficult for a variety of mammalian cells and require several hours if not days to complete.[6]

Molecular Transporters:

A class of compounds known as molecular transporters have recently gained considerable attention for their ability to translocate across the membrane into the cell. First identified from natural proteins such as HIV-1 transcription activator protein (Tat) and the Transcription factor Antennapedia (Antp), they are a class of highly cationic water soluble compounds which maintain their ability to traverse the cell membrane.[7] The HIV Tat protein is able to rapidly enter the cytosol and nucleus of a wide variety of cells by inducing endocytosis.[8] A variety of other proteins have also been discovered with the same ability.[9,10]

Figure 2. Ribbon Structure of HIV-tat

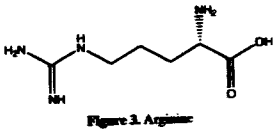

Figure 3. Arginine

In these proteins a small region has been shown to be responsible for the cellular uptake. This region tends to be highly cationic or amphipathic. In Tat the highly cationic region Tat_{49-57} (RKKRRQRRR) has been shown to be primarily responsible for it's cellular uptake.[11] The protein is no longer of capable of entering the cell in the absence of this region. Unlike other proteins capable of entering the cell, the cellular uptake region in molecular transporters retain their activity separate from the protein. It is this unique ability that is showing promise for the delivery of previously unavailable therapeutics into the cell.[8]

Molecular transporters have been shown capable of delivering a wide variety of cargo with sizes up to 500 micrometers. Therapeutics that were otherwise too large, or too polar for the cellular membrane, or too non-polar to travel through the blood stream, would be available for use due to the molecular transporters unique abilities. New target sites with highly polar regions would also become available due to the efficiency of the molecular transporters at cellular uptake and drug delivery. The scope of targeted cells for study would also increase because all previously studied mammalian cell lines have been shown to be receptive to protein transduction. Useful therapeutics, and other cargo unable to cross the cellular membrane could be attached to molecular transporters, carried across the membrane, and then cleanly cleaved from the transporter, free to reach their target site.

Method of internalization:

The mechanism by which molecular transporters cross the cell membrane is still under debate, however multiple theories have been proposed. Early structural studies examined the individual activity of the amino acids in known uptake sequences. Polyhistidine, polyornithine, polylysine and others were found to be ineffective molecular transporters, however polyarginine showed a 20 fold increase in uptake efficiency compared to the natural HIV-Tat sequence. The non-natural D-arginine polypeptide chain showed a 100 fold increase in apparent uptake efficiency, however this is believed to be due to the protease resistance of the poly-D-peptide structure and not due to an increase in uptake efficiency. [12] In examining the structure of arginine, studies showed that a wide variety of structural alterations could be made without significantly affecting the uptake efficiency. A peptide length between 8-16 amino acid residues gives optimal membrane transduction efficiency.[13] A wide variety of backbone structures have been shown to be effective at traversing the cellular membrane. [11] In addition to the natural L-peptides, D-isomer peptides, β-peptides, peptoids, and oligocarbamates have been shown to be effective backbones for molecular transporters despite varying unit lengths, chirality, side chain location, and the inclusion of heteroatoms into the backbone. Molecular transporters with slightly longer side chains have shown increased effectiveness at traversing the membrane, however molecular transporters can have a wide variety of side chain lengths without losing their uptake affinity. [11]

The guanidinium head group of the arginine amino acid side chain is primarily responsible for the cellular uptake of these HIV-Tat based molecular transporters.

While it is a charged moiety capable of hydrogen bonding, those characteristics alone are not sufficient for activity as neither lysine, ornithine, or histidine homopolymers possess the ability to traverse the cellular membrane.[14] It has been suggested by Rothbard *et al.* that it is the ability of the guanidinium moiety to donate a bidentate hydrogen bond that is primarily responsible for its activity. [11] This hydrogen

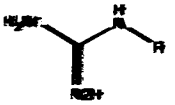

Figure 4. Guanidinium moiety

bonding theory is supported by several studies. Singly N_1-methylated arginine monomers have a decreased in uptake affinity which correlates to the ability of the methyl group blocking the position necessary for hydrogen bond donation. Double N_1-N_1-methylated arginine peptides completely lack the ability to traverse the cellular membrane. [12] A method of internalization proposed by Rothbard, suggests that the guanidinium moiety of the arginine side chain forms bi-dentate hydrogen bond complexes with negatively charged moieties present on the cell surface. Figure 5 shows 3 such complexes which could form. This bi-dentate hydrogen bond interaction between positive and negative moieties is implicated in the uptake as molecular transporters have been shown to have a weaker uptake efficiency in heparin sulfate deficient cell lines. [15] Heparin sulfate is a glycosaminoglycan (GAG) common to the extracellular matrix of

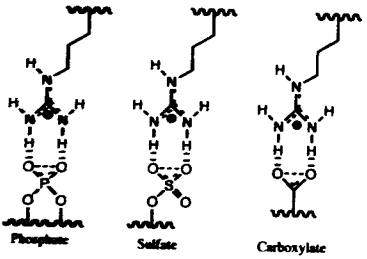

Figure 5. Potential Hydrogen Bonding Complexes for the Guanidinium moiety

mammalian cells involved in a wide variety of life essential and nonessential processes.

Rothbard's theory suggests that the formation of the complex allows for an overall neutral complex which is then capable of passive diffusion through the cell. Contrary to earlier studies passive diffusion no longer appears to be the primary mechanism, although there is still evidence that it still can happen. Fixation artifacts present in earlier studies showed diffuse molecular transporters throughout the nucleus and cytosol. Recent studies done with live cells show that molecular transporters localize in endosomes. The ionic interaction between the guanidinium moieties and the sulfate moieties does appear to be the first step involved in the molecular recognition at the cell surface for stimulating endocytosis[6]. however further research must be carried out in order to gain a better understanding the structural characteristics required for the guanidinium moiety's uptake efficiency.

Hypothesis:

Examination of the guanidinium moiety shows two important characteristics which have not been explored in current literature. Its conjugated structure gives it a highly polarizable nature, as well as an ability to effectively distribute charge. Delocalized π–electrons should have a significant effect due to the uptake mechanism's dependence on the interaction between the molecular transporters and negative cell surface moieties. Any change in the nature of the delocalized π–electrons should have a significant effect in the rate of formation for the necessary complex for cell recognition, ultimately affecting the rate of uptake.

Our Novel Potential Molecular Transporter:

In order to explore this effect, we synthesized a novel peptoid chain containing a guanine pendant side chain with the necessary bi-dentate hydrogen bond donating ability, but with increased conjugation, rendering it more capable of resonance and therefore more polarization. Our compound shown in figure 6 is generated via a convergent synthesis, synthesized separately, and combined yielding our novel compound. An N^9-tethered guanine constitutes the head group of our molecular transporter for direct comparison to the guanidinium moiety of arginine, a peptoid chain constitutes the backbone of our molecular transporter, and a Quantum Dot (QD) fluorophore functions to visualize our peptoids during live cell assays.

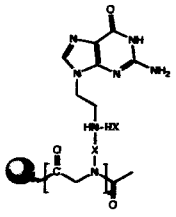

Figure 6. Experimental Potential Molecular Transporter

N^9 Substituted Guanines:

The N^9 substituted guanine structure is shown in Figure 7. It contains the guanidinium moiety, however its conjugated bicyclic nature extends the polarizability and resonance beyond that capable by an isolated guanidinium moiety. Current literature establishes the synthesis of N^9 substituted guanines due to successful biological targeting. N^9 substituted guanines have been explored and several derivatives are currently used for their anti-viral activity.

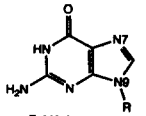

Figure 7. N9 Substituted Guanine

Substitution at the N^9 position is a common motif in these guanine derivatives, however selective substitution has been difficult to achieve. Previous syntheses have relied on steric blocking of the N^9 position.[16] Regiospecific N^9 Michael additions have also been employed with a variety of Michael acceptors which favor the more thermodynamically stable N^9 substitution.[17] However nearly all previous syntheses have relied on chromatography to separate the desired N^9 isomer from the N^7 isomer. Geen et al. fractionally recrystallized the desired N^9 isomer after alkylation by 2-acetoxytetrahydrofuran.[18] Bisachi et al. also use selective crystallization as a key step in a cyclobutyl-substituted guanine in their synthesis of BMS-180194.[19]

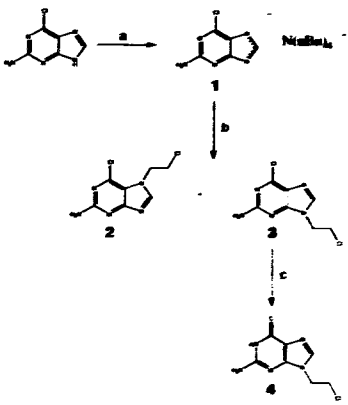

Figure 8. Synthetic Scheme for N^9-(2-chloroethyl) guanine

The synthetic scheme is shown in Figure 8. Synthesis of our N^9 tethered guanine began with commercially available 2-amino-6-chloropurine and is efficiently achieved without employing chromatography. Substitution at the N^9 position is achieved first by the addition of tetrabutylammonium(TBA) hydroxide to quantitatively form the N^9-deprotonated salt of the purine, **1**, as carried out by Bisacchi et al.[20] Once the TBA salt of the guanine has been formed, alkylation at the N9 position is achieved by introducing an excess of 1-bromo-2-chloroethane in a CH_2Cl_2 solution. This yielded a 1:5 ratio of N^7 **(2)**, and N^9 **(3)**, regioisomers. Recrystallization of the crude product in

CH_2Cl_2 yielded the N^9 substituted isomer free from impurity. Hydrolysis of **3** in aqueous HCl yields N^9-(2-chloroethyl)guanine (**4**), in nearly quantitative yield.

In order to test its electrophilicity and show its synthetic versatility in the synthesis of various N^9 substituted guanine derivatives, **4** was reacted with various nucleophiles, yielding derivatives **5-9**. The synthetic scheme for the derivatives is shown in Figure 9. The synthetic versatility of N^9-(2-chloroethyl)guanine is also important in determining the method by which to attach the guaninyl head group to our peptoid backbone.

Many derivatives of **4** were easily synthesized by the introduction of various nucleophiles. The following examples show the versatility of **4** and optimization of yields was carried out by varying the solvent, temperatures and reaction times. Catalytic iodide was used due to its facile displacement of the chloride, resulting in a shorter reaction time for the subsequent derivatives. Synthetic yields were limited by solvation, and so significant effort was spent in determining an appropriate solvent which was polar enough to solvate the N^9-tethered guanine, yet still aprotic and non-polar enough to allow for facile nucleophilic attacks. Temperature increases were significant increasing solvation and

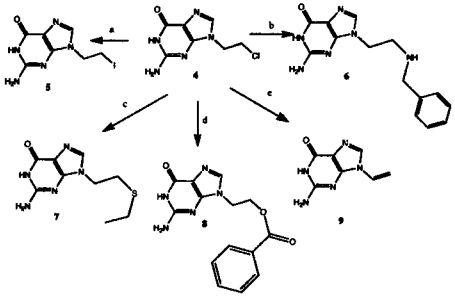

Figure 9. Synthesis of N9-(2-chloroethyl)guanine derivatives:
a. NaI in DMF, 75 C, 1.5 h b.cat NaI, benzylamine in THF, 60 C, 20 h
c. cat NaI , ethanethiol in NaOH & DMSO, 75 C, 1.5 h
d. cat NaI, sodiumbenzoate in DMSO, 120 C, 3.5 h
e. cat NaI, NaOH in DMSO, 85 C, 2 h

in speeding up the reactions to a convenient rate, however competition with the elimination product limited the extent by which the solution could be heated.

Peptoids:

Our lab was interested in synthesizing a novel molecular transporter with high protease resistance to lower the experimental uncertainty introduced by protease degradation in live cells. We also wanted a backbone that had been previously shown to function as a backbone for MT's. Peptoids were chosen due to their increased flexibility in introducing a wide variety of side chain structures, giving increased flexibility in determining the method by which to attach the guanine head group to the backbone. The nitrogen substitution pattern of peptoids introduces too much steric bulk around the amide nitrogens for facile bond cleavage by proteases.[21] The synthesis of the peptoid backbone can be achieved using solid phase synthesis with an orthogonal protecting strategy according to Figure 11. 2-Chlorotritylchloride functionalized polystyrene resin was used as the solid phase anchor for the synthesis. 2-Chlorotritylchloride resin was chosen due to its lability under mild acid conditions, allowing for selective deprotection in the presence of other acid labile protecting groups. Loading of 6-(FMOC-amino) caproic acid allowed for monitoring

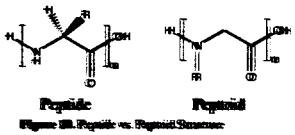

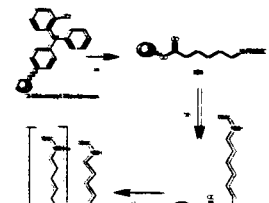

the loading of the resin, while also acting as a spacer to decrease the on-resin steric effects, yielding 5. Excess bromoacetic acid was activated using DIC and then introduced to the resin for the formation of an amide bond. Excess N-Boc-1,6,diaminohexane displaced the bromide on the resin yielding the first residue 11, with a protected side-group preventing any undesired side-reactions. Repeating the introduction of DIC activated bromoacetic acid followed by N-boc-1,6,diaminohexane 8 times gives a peptoid with the desired 9 residues 12. N-capping of the peptoid was achieved with acetic anhydride, preventing any further reaction at the N-terminus 13.

Our amine functionalized Quantum Dot fluorophore was obtained from Evident Technologies, and the attachment protocol for peptide analogues is composed of activating the C-terminus, and introducing the Quantum Dots with their amine functional groups.

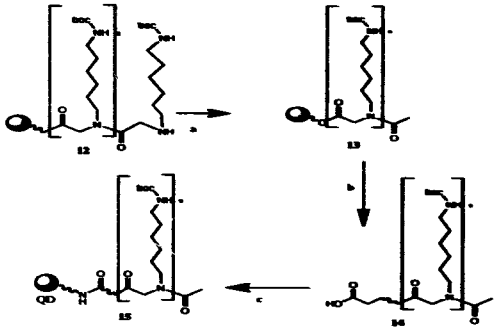

Figure 12. Synthesis of Peptoid Backbone 12-15. a. acetic anhydride b. 0.5 % TFA c. i.DIC, ii. Amine functionalized QD's

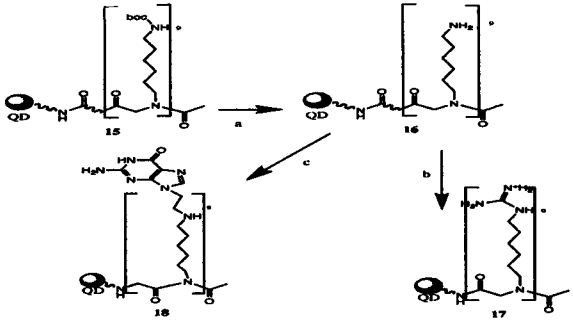

Figure 13. Synthesis of Peptoids 16-18, a. Weak Acid
b. Pyrazole-1-carboxamidine, heat 24 h
c. N9-(2-chloroethyl)guanine

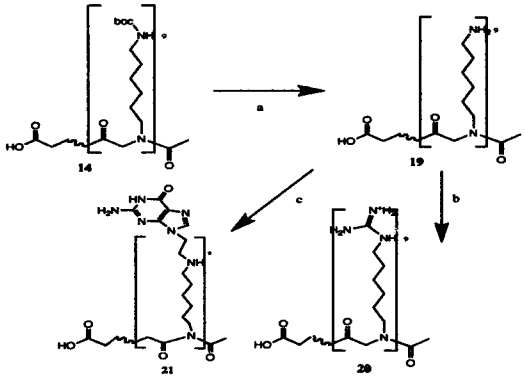

Figure 14. Synthesis of Peptoids 19-21 a. Weak acid
b. Pyrazole-1-carboxamidine, heat 24 h
c. i.DIC, ii. Amine functionalized QD's

For this reason it is necessary to keep the side chains of our peptoid protected until attachment to Quantum Dots, otherwise activation of the C-terminus would result in side chain amine group coupling, instead of the desired coupling with the Quantum Dots.

Cleavage from the 2-Chlorotritylchloride resin was achieved in 0.1% TFA, leaving the Boc protecting groups intact 14. Coupling to the Quantum Dots was carried out according to the Evident technology protocol 15, using size exclusion to filter the excess uncoupled peptoids, and purify our desired Quantum Dot-peptoid complex 16.

After attachment to the Quantum dots, deprotection of the boc protecting group yields a polylysine peptoid analogue 17, which will function as our negative control in our cellular assay. Guanidinylation of 17 was carried out as described by Wender, yielding the polyarginine peptide analogue 18, to function as our positive control in the cellular assay. Synthesis of 19, 20, and 21 the analogues without a QD fluorophore were carried by skipping the Quantum Dot attachment protocol and combining the cleavage from the resin and boc-deprotection into one step. The experimental peptoid 21 was synthesized by nucleophilic attack of 12's side chains on 5 (N^9-(2-chloroethyl)guanine). However further synthetic efforts were delayed by degradation of the 2-Chlorotrityl chloride resin in methylene chloride and DMF. Significant Uv-Absorption occurred after stirring resin in the solvent which is presumed to be due to the trityl group, or the polystyrene fragments.

Cellular assay:

To test the molecular transporter efficiency of our experimental peptoid, multiple different control tests, as well as our experimental peptoid were incubated in MDCK cells and examined by microscopy. Mdacy-Darbin Canine Kidney (MDCK)

cells were used due to their specialization in absorption and secretion. Live cells were observed due to experimental artifacts introduced by fixation.[8]

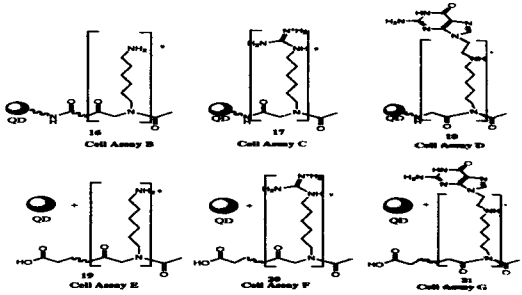

Figure 18. Compounds incubated with cells for Cellular Assays B-G

There are four controls shown in Figure 14 (B,C,E,F)as well as our two experimental (D,G) to determine the molecular transport ability of our experimental peptoid. The cell assay procedure (A-G) involved incubating MDCK cells in a solution containing the compounds of interest (16-21), rinsing the cells after the incubation period has passed, to remove QD fluorescence external to the cell, and then examining the cells by microscopy to determine the quantity and location of the fluorphore within the cells. The first cell assay will be to determine how quantum dots act when they are incubated alone with the cells. Cell assay B consists of incubating 16 with MDCK cells, to act as a standard without molecular transport ability. In cell assay C, we incubate 17 in MDCK cells to act as a standard with known molecular transport affinity. Control tests E, and F were carried out as a comparison to B, and C, differing in that the QD fluorophore is not attached to the

molecular transporter in **D**, and **E**, but is still present in the solution. This will give insight into the different mechanisms by which the molecular transporters function. If **F** results in the cells having the same concentration of quantum dots in the cell as external to the cell, than it would lend evidence that the molecular transporters are disturbing the membrane, and allowing for anything to travel through, which is significantly different than a discreet delivery mechanism. If no quantum dots in **F** are able to enter the cells than it would lend evidence that there is a specific mechanism by which the molecular transporters are able to enter, but which doesn't allow for the entry of anything else. By endocytosis it is also likely that **F** would result in a small amount of quantum dots present in the cells that were nearby and were pinched off into the cells when endocytosis occurred. Cell assay **D**, will give insight into the molecular transport efficiency of our novel peptoid, with high internal quantum dot concentrations corresponding to a high molecular transport ability, and low internal quantum dot concentration corresponding to low molecular transport ability. Cell assay **C** will give information on whether our compound functions any differently than **20** and **17** in Assays **C** & **F**.

EXPERIMENTAL

General

All purchased reagents were used without further purification. Thin-Layer Chromatography (TLC) was performed on Selecto Scientific Silica Gel 60, F-254 TLC plates. Melting points were obtained using a Laboratory Devices MEL-TEMP and are uncorrected. ^{1}H-NMR spectra were obtained using a Varian Gemini-200 (200 MHz). Chemical shifts are reported as δ in ppm referenced to the solvent residual peak of DMSO-d_6 (δ 2.50) unless otherwise noted.

N9-(2-chloroethyl)guanine;

Tetrabutylammonium 2-amino-6-chloropurin-9-ide (1). Procedure was adapted from Bisacchi *et al.* Aqueous tetrabutylammonium hydroxide (~1.5 M, 39.3 mL, ~59 mmol) was added to a slurry of 2-amino-6-chloropurine (10.0 g, 59 mmol) in 250 mL of CH_2Cl_2. The reaction mixture was stirred for 30 min and the solvent removed *in vacuo*. Concentration from toluene (3 × 100 mL) allowed for the removal of water and resulted in crystallization. The solid was triturated with 200 mL of ether, filtered, washed with ether, and dried under vacuum over $CaSO_4$ to yield **1** (24.4 g, 59 mmol, 100%). The orange solid was used without further purification: mp 66-70 °C; R_f = 0.60 ($CHCl_3$/EtOAc/EtOH 1:1:1); ^{1}H-NMR (DMSO-d_6), referenced to TMS δ 0.00) δ 0.92 (12H, t), 1.28 (8H, m), 1.58 (8H, m), 3.16 (8H, m), 6.38 (2H, s), 7.55 (1H, s). ^{13}C-NMR (DMSO-d_6, δ): 167.0, 157.8, 156.6, 145.4, 128.0, 58.5, 24.0, 20.1, 14.4.

N^7- and N^9-(2-chlororoethyl)-2-amino-6-chloropurine (2, 3). To a solution of **1** (10.0 g, 24 mmol) in 30 mL of CH_2Cl_2 was added 1-bromo-2-chloroethane (10 eq, 19.9 mL, 240 mmol). The reaction mixture was stirred at 60°C for 2 h, during which time precipitation occurred. The solid was filtered, washed with cold CH_2Cl_2, and dried under vacuum over $CaSO_4$ to yield a 1:5 mixture of **2** and **3** (4.78 g, 20 mmol, 85% combined yield). Recrystallization from CH_2Cl_2 (~20 mL) provided 3.70 g of the N9 isomer, **3**, free of contamination with N7 isomer **2**: mp 189-191 °C; R_f = 0.65 ($CHCl_3$/EtOAc/EtOH 1:1:1); ^{1}H-NMR (DMSO-d_6) δ 4.04 (2H, t), 4.41 (2H, t), 6.99 (2H, s), 8.17 (1H, s). Compound **2**: R_f = 0.49 ($CHCl_3$/EtOAc/EtOH 1:1:1); The ^{1}H-NMR spectrum of **3** was consistent with that reported previously. ^{1}H-NMR (DMSO-d_6) δ 8.17 (1H, s), 6.977 (2H, s), 4.42 (2H, m), 4.05 (1H, m). ^{13}C-NMR (DMSO-d_6, δ): 159.8, 154.1, 149.5, 143.3, 123.3, 44.8, 42.5. MS *m/z* (relative intensity): 231.0 (56%), 196.0 (22%) 169.0 (100%), 146.0 (16%), 134.0 (45%), 84.0 (39.0%), 66.0 (48%). HRMS (*m/z*): $[M]^+$ calcd for $C_7H_7N_5Cl_2$, 231.0079; found, 231.0083.

N^9-(2-chloroethyl)guanine (4). A solution of 3 M $HCl_{(aq)}$ (13 mL), containing **3** (2.5 g, 10.8 mmol), was refluxed for 1 h. The solution was cooled to rt and neutralized with saturated $NaHCO_{3(aq)}$. The resulting solid was filtered, washed with cold water, and dried under vacuum over $CaSO_4$ to yield **4** (2.31 g, 10.8 mmol, 100%): mp >250 °C; R_f = 0.24 ($CHCl_3$/EtOAc/EtOH 1:1:1); ^{1}H-NMR (DMSO-d_6) δ 3.97 (2H, t), 4.29 (2H, t), 6.53 (2H, s), 7.74 (1H, s), 10.70 (1H, s). MS *m/z* (relative intensity): 213.0 (100%), 177.0 (28%) 151.0 (96.5%), 109.0 (63.0%). HRMS (*m/z*): $[M]^+$ calcd for $C_7H_8ON_5Cl$, 213.04174; found, 213.04192.

N^9-(2-iodoethyl)guanine (5). A solution of 4 (100 mg, 0.468 mmol) containing NaI (10 eq, 701 mg, 4.68 mmol) in DMF (2-3 mL) was stirred at 75 °C for 1.5 h. The DMF was removed under vacuum. The resulting solid was triturated with water, filtered, washed with water, and dried under vacuum over $CaSO_4$ to yield 5 (110 mg, 0.361 mmol, 77%): mp >250 °C; ^{1}H-NMR (DMSO-d_6) δ 3.56 (2H, t), 4.29 (2H, t), 6.49 (2H, s), 7.72 (1H, s), 10.59 (1H, s). MS *m/z* (relative intensity): 304.9 (1%), 253.7 (16%), 177.0 (10%), 127.9 (100%) 91.0 (8%), 63.4 (7.5%) HRMS (*m/z*): $[M]^+$ calcd for $C_7H_9ON_5I$ 304.9774; found, 304.9778.

2-amino-9-(2-(benzylamino)ethyl)-1*H*-purin-6(9*H*)-one (6). Benzylamine (4 eq, 1.87 mmol 204 μL) was added to a solution of 4 (100 mg, 0.469 mmol) containing NaI (21 mg, 0.140 mmol) in THF (~5 mL). The solution was then stirred for 20 h at 60 °C. After cooling the reaction mixture to rt, acetone (~20 mL) was added, resulting in precipitation. The solid was filtered, washed with acetone, and dried under vacuum over $CaSO_4$ to yield 6 (112 mg, 0.394 mmol, 84%): ^{1}H-NMR (DMSO-d_6) δ 3.24 (2H, t), 4.11 (1H, s), 4.28 (2H, t), 6.66 (2H, s), 7.43 (5H, m), 7.70 (1H, s), 8.77 (1H, s), 10.76 (1H, s).

2-amino-9-(2-(ethylthio)ethyl)-1*H*-purin-6(9*H*)-one (7). NaI (21 mg, 0.140 mmol) and 4 (100 mg, 0.468 mmol) were added to a solution of NaOH (4 eq, 1.87 mmol, 75 mg) and ethanethiol (4 eq, 1.87 mmol, 138 μL) in DMSO (1 mL). The resulting solution was stirred at 75 °C for 1 h and then cooled to rt. Water (~20 mL) and

glacial acetic acid (0.1 mL) were added until precipitation occurred. The resulting solid was filtered, washed with water, and dried under vacuum over $CaSO_4$ to yield **7** (66 mg, 0.276 mmol, 59%): ^{1}H-NMR (DMSO-d_6, referenced to HOD δ 3.30) δ 1.09 (3H, t), 2.45 (2H, q) 2.82 (2H, t), 4.05 (2H, t), 6.39 (2H, s), 7.64 (1H, s), 10.51 (1H, s). ^{13}C-NMR (DMSO-d_6) δ 157.9, 154.5, 152.1, 138.7, 117.4, 43.4, 31.1, 25.6, 15.6, MS *m/z* (relative intensity): 307.1 (8.5%), 239.0 (76%), 210.0 (32%), 179.0 (79%), 151.0 (100%), 109.0 (40%), 89.0 (58%), 62.0 (48%) HRMS (*m/z*): $[M]^+$ calcd for $C_9H_{13}ON_5S$ 239.0841; found, 239.0838.

2-(2-amino-6-oxo-1*H*-purin-9(6*H*)-yl)ethyl benzoate (8). A solution of **4** (100 mg, 0.468 mmol) containing NaI (21 mg, 0.140 mmol) and sodium benzoate (4 eq. 1.87 mmol, 270 mg) in DMSO-d_6 (2-3 mL) was stirred at 120-130 °C for 3.5 h. Water (~20 mL) was added to the hot reaction mixture and a precipitate formed. The solid was filtered, washed with water, and dried under vacuum over $CaSO_4$ to yield **8** (54 mg, 0.180 mmol, 39%): R_f = 0.32 ($CHCl_3$/EtOAc/EtOH 1:1:1); ^{1}H-NMR (DMSO-d_6) δ 4.36 (2H, t), 4.56 (2H, t), 6.47, 7.50 (2H, t), 7.65 (1H, t), (2H, s), 7.77 (1H, s), 7.91 (2H, d), 10.58 (1H, s). ^{13}C-NMR (DMSO-d_6) δ 165.5, 157.0, 153.8, 151.5, 139.9, 137.9, 133.6, 129.4, 128.9 (C_{12}), 116.6, 63.1, 42.0, MS *m/z* (relative intensity): 299.0 (12.0%), 179.0 (20.0%), 165.0 (35.5%), 152.0 (30.0%), 133.1 (12.5%), 105.0 (27.5%), 91.0 (100%), 66.0 (68.5%). HRMS (*m/z*): $[M]^+$ calcd for $C_{14}H_{13}O_3N_5$ 299.10185; found, 299.10157.

2-amino-9-vinyl-1*H*-purin-6(9*H*)-one (9). A solution of **4** (100 mg, 0.468 mmol) containing NaI (21 mg, 0.140 mmol) in DMSO (1 mL) was treated with NaOH (4 eq, 1.87 mmol, 75 mg) and stirred at 75-85 °C for 1.5 h. The resulting precipitate was cooled to rt and dissolved in water (~5 mL). Precipitation occurred following addition of glacial acetic acid (~1 mL). The purple solid was filtered, washed with water, and dried under vacuum over $CaSO_4$ to yield **9** (68 mg, 0.384 mmol, 82%): ^{1}H-NMR (DMSO-d_6) δ 5.02 (1H, d), 5.85 (1H, d), 6.57 (2H, s), 7.05 (1H, q), 8.08 (1H, s), 10.73 (1H, s). ^{13}C-NMR (DMSO-d_6) δ 157.0, 154.3, 150.4, 134.7, 126.9, 102.9, 96.6, 22.6. MS *m/z* (relative intensity): 177.0 (81.0%), 78.0 (82.0%), 62.9 (100%) HRMS (*m/z*): $[M]^+$ calcd for $C_7H_7ON_5$ 177.06507; found, 177.06501.

Peptoid Backbone:

General: 2-chlorotrityl Chloride resin was purchased from NovaBiochem. Quantum Dots were obtained from Evident Technologies. Spin filters were obtained from the Union Biology Department.

Synthesis of lysine peptoid analogue with Boc-protected side chains (14).

A sub-monomer approach was employed in peptoid synthesis. Peptoids were manually synthesized in fritted vessels using mechanical agitation to ensure mixing. A chloranil test for secondary amines was performed after each completion of a residue to test for the presence of secondary amines. Agitation of the 2-chlorotrityl Chloride resin (45.5 mg) in DCM (4-5 ml) for 30 minutes exposed approximately 50

µmol of trityl functional group. Treatment of the exposed trityl group with DCM/MeOH/DIPEA (17:2:1, 2-3 ml) yielded the active resin. The resin was then washed with DCM (2-3 ml x3), then DMF (2-3 ml x3) and again with DCM (2-3 ml x3) before being treated with a solution of 6-(N-FMOC)caproic acid (20 eq) and DIC (26 eq) in DCM (4 ml) to yield **10**. The resin was then washed again with DCM (2-3 ml x3), then DMF (2-3 ml x3) and again with DCM (2-3 ml x3). Treatment with 20% (v/v piperidine/DMF (1-2 ml for 1 min, 2-3 ml x 5 for 10 min, and 2-3 ml for 10 min) to yield an exposed amine group. UV-vis was used on the wash solution to determine loading effectiveness. The resin was then washed with DCM (2-3 ml x3), then DMF (2-3 ml x3) and again with DCM (2-3 ml x3). A solution of bromoacetic acid (20 eq) and DIC (26 eq) in DCM (4 ml) was added to the resin and agitated for 45 minutes. The resin was then washed with DCM (2-3 ml x3), then DMF (2-3 ml x3) and again with DCM (2-3 ml x3). A solution containing *N*-Boc-1,6-hexanediamine (17 eq) in DCM (4 ml) was agitated for 45 minutes to yield **11**. The resin was then washed with DCM (2-3 ml x3), then DMF (2-3 ml x3) and again with DCM (2-3 ml x3). The bromoacetic acid and amine substitution steps were repeated until a 9-residue oligomer, **12**, had been obtained. A solution of Acetic Anhydride 5% (v/v) in DMF was added to the resin and agitated for 45 minutes to yield **13**. The resin was then washed with DCM (2-3 ml x3), then DMF (2-3 ml x3) and again with DCM (2-3 ml x3). Treatment of the resin with 0.1 % TFA in DMF at 0°C for 4 hours yielded **14**. TFA was removed *in vacuo* and the crude oil was triturated with cold ether (20 ml) and centrifuged. The ether was removed by decantation. HPLC analysis showed little impurity and so no further purification was used.

Quantum Dot Conjugation to Peptoids (15).(Proposed)

Conjugation to he Quantum Dots was achieved by the Evident Technologies Protocol. **14** was dissolved in a phosphate buffer system (PBS) (1 ml, pH 7.00) with EDC (5000 eq.). The Quantum Dot solution (~0.1 ml, 12:1 peptoids : Quantum Dots ratio) was added to the peptoid solution. 10x PBS (0.05 ml) was then added to solution. Deionized water was then added until the total solution volume reached 0.5 ml. The peptoids were then incubated with agitation for 2.5 hours to yield **15**. Weight discriminatory spin filters (10 min) separated the unconjugated peptoids, from the Quantum Dot conjugated complex. Rinsing with H_20 (0.3 ml x2) with spin filtering yielded pure peptoids.

Polylysine peptoids with and without Quantum Dots attached (16, 19).(Proposed)

A solution of **15** (1 ml, 50 μmole) in H_20 with Acetic Acid (1 M, 0.1 ml) yields **16**. Treatment of **14** (1 ml, 50 μmole) in H_20 with Acetic Acid (1 M, 0.1 ml) yields **19**. Remove acetic acid *in vacuo* and triturate the crude oil with cold ether (20 ml) and centrifuge. Decant the cold ether

Polyarginine Peptoids with and without QD's (17, 20).(Proposed)

Perguanidinylation of **16** and **19** will be carried out as described by Wender *et al.*[28] to yield **17** & **20** respectively.

Guanine side-chain Peptoids with and without QD's (18, 21). (Proposed) **Guaninylation of 16 and 19** will be carried out by stirring a solution of **16** and **19** with **N9-(2-chloroethyl)guanine (4)** (10 eq) containing NaI (21 mg, 0.140 mmol) in **THF** (~5 mL). The solution was then stirred for 20 h at 60 °C. After cooling the reaction mixture to rt, add acetone (~20 mL), resulting in precipitation. Filter the solid, wash with acetone, and dry under vacuum over $CaSO_4$.

Synthesis:

N^9-(2-chloroethyl)guanine:

Our easily scalable synthesis which is able to avoid chromatography and blocking groups for alkylation allowed for an efficient synthesis of N^9-(2-chloroethyl)guanine with an overall yield of 58%. N^9-(2-chloroethyl)guanine was also shown to be a versatile reagent in synthesis of other N^9-substituted guanines.

N^9-(alkyl)guanine derivatives:

N^9-(2-chloroethyl)guanine reacted readily with various nucleophiles. The Finkelstein reaction readily yielded the corresponding iodo form, 5, in high yield (77%), and so NaI was used as a catalyst in the subsequent reactions. 6 readily formed by substitution with a primary amine (benzyl amine) in high yield (84%) and shows promise for the intended pathway for guaninylation of the peptoids to yield 18 and 21. 7 and 8 were also formed in good yield by substitution with a thiol (59%), and benzoate (39%), respectively. The elimination product 9, (82%) also readily formed in high yield. The solvent played a large role in determining the rate of reaction. The polarity of guanine requires a polar solvent, which indirectly affects the rate of reaction. Significant optimization of the reactions occurred in determining an appropriate solvent to carry out the reactions. Temperature also proved an important factor in optimizing yields of these reactions however competition with elimination limited the extent to which the reaction could be heated. The model chemistry showed that N^9-(2-chloroethyl)guanine is a versatile reagent which could be used in the synthesis of a wide range of N^9- substituted guanines.

Peptoid Synthesis:

The synthesis of our peptoids is based on a submonomer approach with orthogonal protection scheme allowing for the inclusion of a wide variety of side-chains into the peptoid structure as well as selectivity and control in determining the location of the functional groups affected by the reactions. This allows us to build our peptoids off of the N-terminus of the peptoid. coupling bromoacetic acid to the N-terminus amine, without affecting the side-chain amines. Selectivity in this step was critical for building our linear peptoids. Selective coupling of the C-terminus carboxylate group to the amino functionalized quantum dots is also critical to our synthesis. The orthogonal protecting scheme allows the C-terminus to selectively react with the amino groups attached to the quantum dots. Without the protecting groups, the activated ester would favor coupling to a side chain amino group, which is more immediately available and present in higher concentration than the quantum dot amino groups.

The 2-chlorotrity Chloride resin was chosen as the solid-phase anchor for the peptoid synthesis due to its lability under mildly acidic conditions. Its mild lability allowed the use of the boc protecting group on the side chains, which must remain unaffected by the cleavage from the resin. The resin was expected to act as a stable anchor, however UV-Vis spectroscopy of DMF and CH_2Cl_2 solutions stirred with resins showed evidence of degradation, possibly fragments of polystyrene or trityl groups. This emphasizes the importance of examining the progress of the reactions over the course of the peptoid synthesis.

FMOC de-protection allows for UV-Vis examination of the solution for the presence of the dibenzofulvene adduct. In our synthesis this was used to test the

effectiveness of the 6-(N-FMOC)caproic acid loading onto the resin. The Chloranil test, which is effective at detecting the presence of primary and secondary amines, can be used to determine the effectiveness in building each section of the residues. A negative test after carrying out the nucleophilic attack of 1,6-FMOC-diaminohexane on the peptoid residue, shows the successful conversion into the secondary amine in the backbone. A negative test result after coupling bromoacetic acid onto the peptoid chain shows successful conversion into the backbone amide.

The N-terminus was capped with bromoacetic acid to prevent any side reactions during the rest of the synthesis. This was designed to prevent any coupling of the N-terminus to other activated C-termini during the quantum dot coupling step, but applies to any reactions after the desired number of residues have been synthesized, involving the N-terminus.

Coupling the peptoid to the quantum dot was carried out with the peptoids in slight excess. There is an average of 10 amino functional groups present on Fort Orange amine QD's, and so 12 equivalents of peptoids were added per quantum dot in the synthesis of compound 15. It was important to ensure that all of the quantum dots were coupled to peptoids due to the extremely difficult task of separating the conjugated quantum dots from the unconjugated quantum dots. Any uncoupled peptoids can easily be separated from the quantum dot complexes using a mass discriminatory spin filter. The large mass of the quantum dots complexes provides a simple method for purification from the much smaller side products of the subsequent reactions which yield 16, 17, and 18.

Perguanidinylation of the peptoids has been carried out on **19** to yield **20**., but has not yet been carried out on **16** to yield **17**. Purification of **20** was carried out by RPLC . and significant time could be saved by determining a smoother method. **17** has not yet been synthesized, however due to its large mass, a weight discriminatory spin filter is expected to provide an acceptable purification method. This same method is expected to be efficient in the purification of the guaninylated peptoid **18**, however it is expected that RPLC will have to be used to purify **21**.

Cellular Assays:

There are 7 different tests (A-G) which should be carried to assess the ability of the guaninylated peptoids **18** and **21** to enter the cell. The cell assay procedure involves incubating MDCK cells in a solution containing the compounds of interest (**16-21**). rinsing the cells after the incubation period has passed, to remove QD fluorescence external to the cell, and then examining the cells by microscopy to determine the quantity and location of the fluorphore within the cells. In the preliminary tested carried out so far microscopy was used to determine the location of the QD's. Assay A. contains a solution of quantum dots to assess their activity when incubated with the cells alone. Assays B-G each contain one of the peptoid compounds synthesized (**16-21**). Cells assays E-G. which contain compounds **19-21**, have a solution of quantum dots added to yield the same concentration of fluorophore as Assays A-D.

Figure 15 shows the results from Assay A when carried out on interior MDCK cells. Examination of the images show that no quantum dots appear to have entered

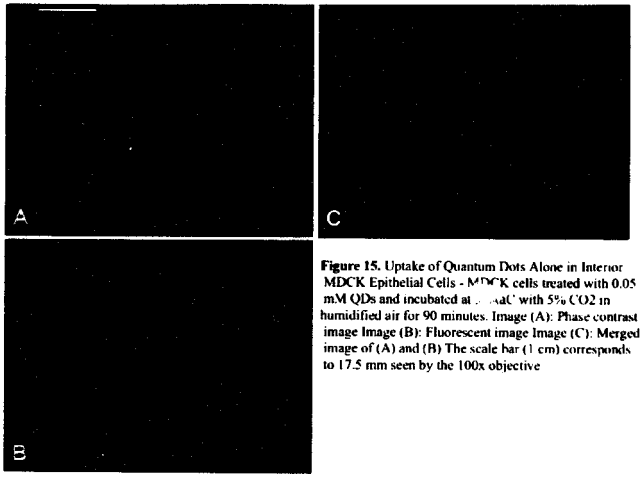

Figure 15. Uptake of Quantum Dots Alone in Interior MDCK Epithelial Cells - MDCK cells treated with 0.05 mM QDs and incubated at 37°C with 5% CO2 in humidified air for 90 minutes. Image (A): Phase contrast image Image (B): Fluorescent image Image (C): Merged image of (A) and (B) The scale bar (1 cm) corresponds to 17.5 mm seen by the 100x objective

the cells. This can be inferred due to the differences in focus. The focus of the microscope is aligned upon the cells, and any quantum dots in focus are considered being in the same level as the cells, while those out of focus are above or below the cells. Any quantum dots found in focus in the same spot as a cell could only be there because it is inside the cell. Out of focus quantum dots in the same spot as cells are above or below, but not inside the cell. Examination of Image C in Figure 15 shows that there does not appear to be any quantum dots that could be considered inside the cells. This figure shows that in the subsequent assays, any cells which contain quantum dots within them, is due solely to the activity of the peptoids attached to them, as quantum dots are

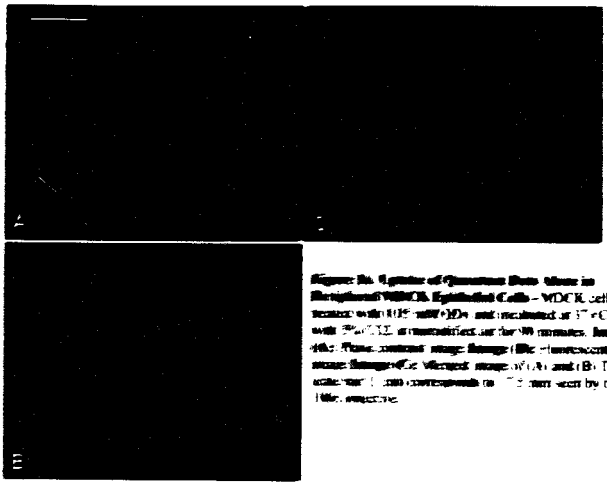

incapable of entering the cells on their own. Figure 16 shows a second run of Cell Assay A with periphery MDCK cells, which gives the same result, leaving no quantum dots present within the cell. Figure 16 does differ from Figure 15 in that there appears to be some quantum dots attached to the sides of the cells, but this is expected considering the large number of negative cell surface moieties and the positive amine groups present on the quantum dot surface. The quantum dots are still on the exterior of the cell, and so this shows further evidence that the quantum dots can not enter the cells.

The cell assays **B-D** and **G** have not yet been carried out due to the chloromethyl chloride resin degradation delaying the peptoid synthesis plans, however Cells Assays **E** and **F** have been carried out and show promising results.

Figure 17 shows the results from Cell Assay **E**. Examination of the cells shows the quantum dots non-specifically bound to the cell membrane of the cells, however no quantum dots appear to have entered the cells.

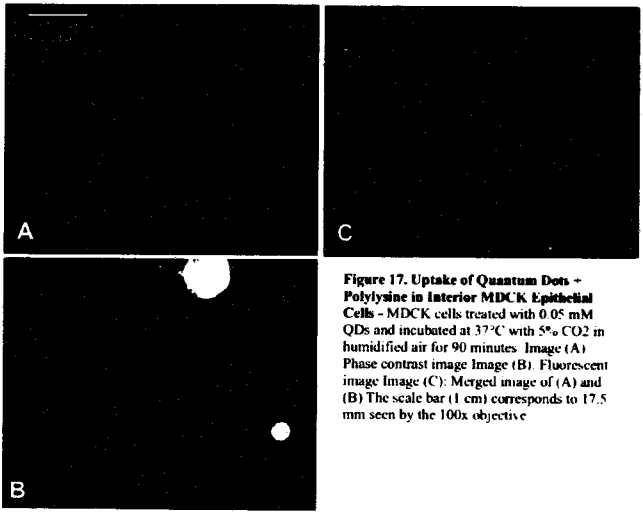

Figure 17. Uptake of Quantum Dots + Polylysine in Interior MDCK Epithelial Cells - MDCK cells treated with 0.05 mM QDs and incubated at 37°C with 5% CO2 in humidified air for 90 minutes. Image (A) Phase contrast image Image (B). Fluorescent image Image (C): Merged image of (A) and (B) The scale bar (1 cm) corresponds to 17.5 mm seen by the 100x objective

This shows that compound **19** provides a good negative for the test because no quantum dots were able to enter the cells. We are unable to see the peptoids themselves, however this shows that the poly lysine does not appear to induce endocytosis, which would result in some quantum dots entering the cells. This provides a good contrast for the subsequent assays for comparison to Assays **F** & **G** with compounds **20** and **21**.

Figure 18 shows the results from Cell Assay F.

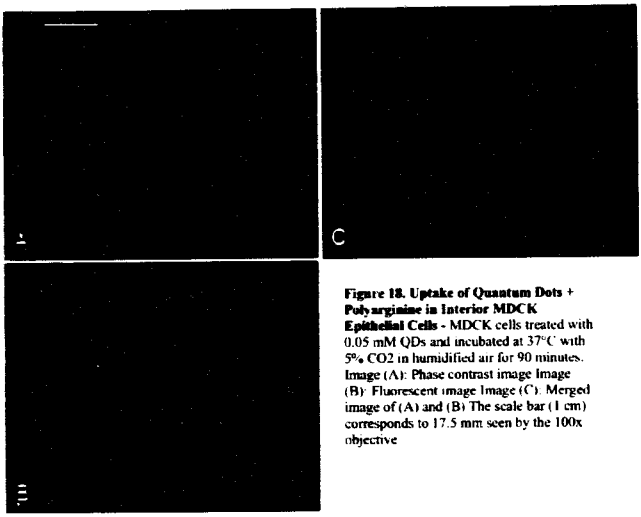

Figure 18. Uptake of Quantum Dots + Polyarginine in Interior MDCK Epithelial Cells - MDCK cells treated with 0.05 mM QDs and incubated at 37°C with 5% CO2 in humidified air for 90 minutes. Image (A): Phase contrast image Image (B): Fluorescent image Image (C): Merged image of (A) and (B) The scale bar (1 cm) corresponds to 17.5 mm seen by the 100x objective

We are unable to see the peptoids in this assay, and so we can not yet speculate on their location in the cell, however this cell assay offers encouraging results due to the presence of some quantum dots within the cells. This suggests that the peptoids are inducing endocytosis. The endocytosis traps quantum dots which are nearby, resulting in their entry into the cells. The differences between this assay and cell Assay E will provide a good basis for determining the efficiency, and possibly any differences in delivery mechanism.

References:

1. Pratt, C. W.; Cornelly K.; Essential Biochemistry, **2004**. Wiley
2. Kelly, J. L.; Krochmal, M.P.; Scaeffer, H.J., Purine acyclic nucleosides. Nitrogen isosteres of 9-[(2-hyroxyethoxy)methyl] guanine as candidate antivirals. *J. Med Chem.* **1981,** *24*, 1528-1531.
3. Denicourt, C.; and Dowdy, S.F. Protein transduction technology offers novel therapeutic approach for brain ischesmia, Trends Pharmacol. Sci. **2003** *24*. 216-218
4. Leifert, J.A. and Lindsay Whitton, J.) "Translocatory Proteins" and "protein transduction Domains: a critical analysis of their biological effects and underlying mechanisms, *Mol/ Ther.* **2003,** 8, 13-20
5. Schwarze, S.R.; Hruska, K. A.; Dowdy, S.F.) Protein Transduction: unrestricted delivery into all cells? *Cell Bio.* **2000,** 10, 290-295
6. Thierry, A. R.; Vives, E., Richard, J. P. Prevot, P., Martinandonni, C., rabbins,I., and Lebleu, B. Cellular uptake and intracellular fate of antisense oligonucleotides. *Curr. Opin. Mol. Ther.* (**2003**) *5*, 133- 138.
7. Martin,J.C.;Jeffrey, G.A.; McGee, D.P.C.; Tippie, M. A.; Sance, D.F.; Mathews, T.R.; Verheyden, J.P.H., Acyclic analogs of 2'-deoxynucleosides related to 9-[(1,3-dihydroxy-2-propoxy)methyl]guanine as potential antiviral agents. *J. Med Chem.* **1985,** *28*. 358-362
8. Fuchs, M.S.; Raines, R.T.; Pathway for Polyarginine Entry into Mammalian Cells. *Biochemistry*, **2004,** 43. 2438-2444
9. Kim, C.V.; Luh, B.Y.; Martin, J.C. Synthesis and antiviral activity of (S)-9-[4-hydroxy-3-(phosphonomethoxy)butyl]guanine *J. Med Chem* **1990**, *33*. 1797-1800
10. Hakimelahi, G.H.; Ly, T.W.; Moosavi-Movahedi, A.A.; Jain, M. L.; Zakerinia,M.; Davari, H.; Mei,H.; Sambaiah, T.; Moshfegh, A.A.; Hakimelahi, S. Design, Synthesis, and Biological Evaluation of Novel Nucleoside and Nucleotide Analogues as Agents against DNA Viruses and/or Retroviruses. *J. Med Chem.* **2001**, *44*, 3710-3720.
11. Rothbard,J.B.; Jessop, T.C.; Lewis, R.S.; Murray, B.A., Wender, P.A.; Role of Membrane Potential and Hydrogen Bonding in the Mechanism of Translocation of Guanidinium-Rich Peptides into Cells, *J. ACS*, **2004.**
12. Futaki, S. et. al. Arginine-rich peptides: An abundant source of membrane-permeable peptides having potential as carriers for intracellular protein delivery. *J.biol Chem*, 2001, **276(8)**: p. 5836-40
13. Wender, P.A.; Mitchell, D.J.; Pattabiraman, K.; Pelkey, E.T.; Steinman, L.; and Rothbard, J.B.; **2000**. *97*. 13003-13008.
14. Derossi, D.; Joliot, A. H.; Chassaing. G.; Prochiantz. A. The third helix of the Antennapedia homeodomain translocates through biological membranes *J Biol. Chem.* **1994**, *269*, 10444-10450
15. Goncalves, E., Kitas,E. et al. **(2005)**. Binding of oligoarginine to membrane lipids and heparin sulfae: structural and thermodynamic characterization of a cell-penetrating peptide." Biochemistry, *44(7)*: 2692-2702

16. Torii, T.; Shirigami,H.; Yamashita, K.; Suzuki,Y.; Hijiya, T.; Kashiwagi, T.; Izawa, K. Practical Synthesis of penciclovir and famciclovie from N2-acetyl-7-benzylguanine. *Tetrahedron*, **2006**, article in press
17. Geen, G.R.; Kincey,P.M.; Choudary,B.M. Regiospecific Michael Additions with 2-amino purines. Tetrahedron Lett. 1992, 33, 4609-4612
18. Geen, G.R.; Kincey, P.M.; Spoors, P.G. Regioselective alkylation of guanines using 2-acetoxytetrahydrofurans. Tetrahedron Lett. 2001, 42, 1781-1784.
19. Bisacchi, G.S.; Geen,G.R.; Ramsay, T.W.;Share, A.C.; Slater, G. R.; Smith, N. M. Tetrahedron **2000**, *56*, 4589-4595
20. Bisacchi, G.S.; Singh,J.; Godfrey, Jr., J.D.; Kissick,, T.P.; Mitt, T.; Malle, M.F.; Di Marco, J.D.; gougoutas, J.Z. ; Mueller, R.H.; Zahler, R. Regioselective Coupling of Tetraalkylammonium salts of 6-iodo-2-aminopurine to a Cyclobutyl Triflate: Efficient Preparation of homochiral BMS-180,194, a Potent Antiviral Carbocyclic Nucleoside, *J. Org. Chem*, 1995, 60, 2902-2905.
21. Murphy, J.E.; Uno,T.; Hamer, J.D.; Cohen, F.E.; Dwarki, V.; Zuckerman, R.N.; *A combinatorial approach to the discovery of efficient cationic peptoid reagents for gene delivery*, PNAS, **1998**(95), 1517-1522.
22. Huryn, D.M.; Okabe, M.; AIDS driven nucleoside chemistry, *Chem Rev.* **1992** *92*, 1745-1768
23. Franchetti, P.; Sheikha, G.A.; Capellacci, L.; Grifantini, M,; De Montis, A,; Piras, G.; Loi, A.G.; La Colla, P. *J. Med. Chem.* **1995**, *38*, 4007-4013
24. Bonetta, L. *The Scientist* **2002**, *16*, 38
25. Frankel, A. D.; Pabo, Cc.O. *Cell* **1988**, *55*, 1189-1193
26. Krenitsky, T.A.; Hall, W.W.; De Miranda, P.: Beauchamp, L.M.; Schaffer, H.J.; Whiteman, P.D.;Proc. Natl. Acad. Sci. USA **1984**, *81*, 3209-3213.
27. Miller S M, Simon R J, Ng S, Zuckermann R N, Kerr J M, Moos W H. Drug Dev Res. 1995;35:20–32
28. Wender, P.A.; Mitchell, D.J.; Pattabiraman, K.; Pelkey, E.T.; Steinman, L.; Rothbard,B.J.; The design, synthesis and evaluation of molecules that enable or enhance cellular uptake: Peptoid molecular transporters, *PNAS*, **2007**, *97*, 13003-13008.

Figure Appendix

Figure 1. Cartoon of Cell Membrane

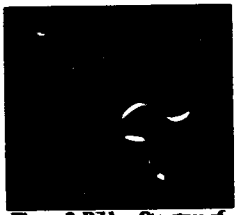

Figure 2. Ribbon Structure of HIV-tat

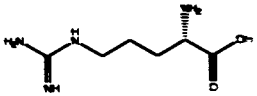

Figure 3. Arginine

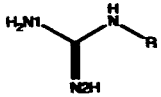

Figure 4. Guanidinium moiety

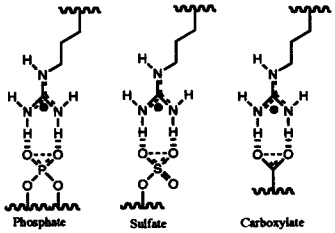

Figure 5. Potential Hydrogen Bonding Complexes for the Guanidinium moiety

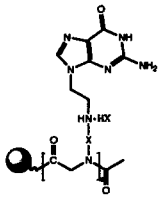

Figure 6. Experimental Potential Molecular Transporter

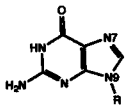

Figure 7. N9 Substituted Guanine

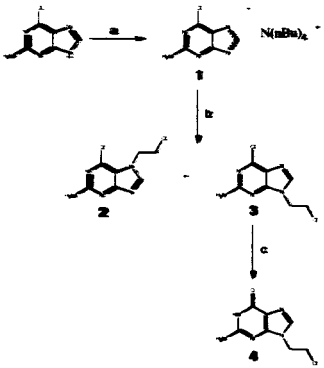
N(nBu)4
1
2
3
4

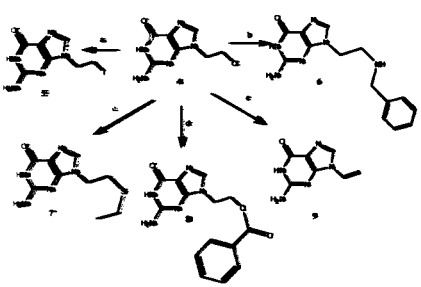


Peptide
Peptoid

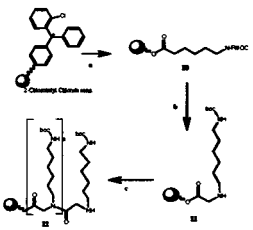

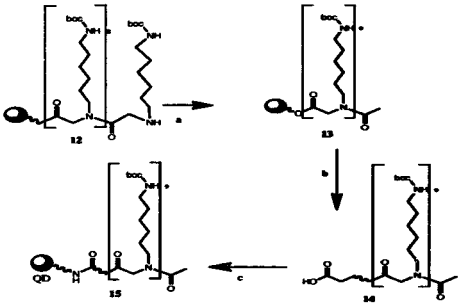

Figure 12. Synthesis of Peptoid Backbone 13-15. a. acetic anhydride
b. 0.5 % TFA
c. LDIC, d. Amine functionalized QDs

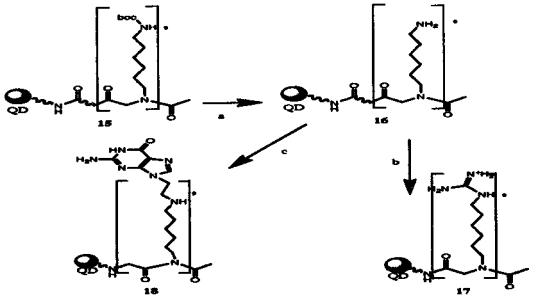

Figure 13. Synthesis of Peptoids 15-18, a. Weak Acid
b. Pyrazole-1-carboxamidine, heat 24 h
c. N9-(2-chloroethyl)guanine

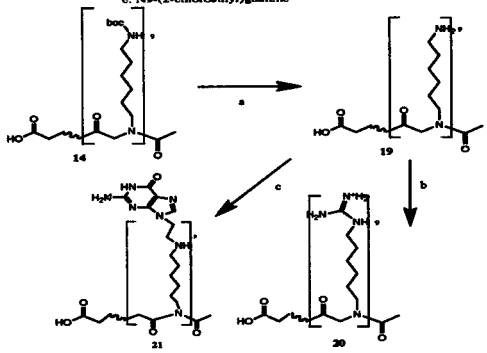

Figure 14. Synthesis of Peptoids 19-21 a. Weak acid
b. Pyrazole-1-carboxamidine, heat 24 h
c. i.DIC, ii. Amine functionalized QD's

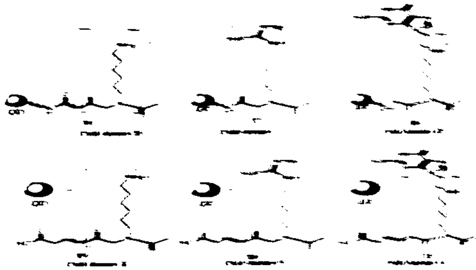

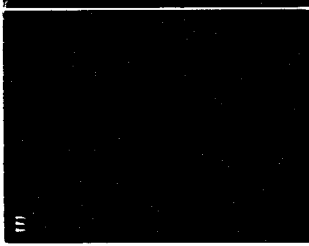

Figure 55. Images of Quantum Dots Alone in Interior of MDCK Epithelial Cells. MDCK cells treated with 0.05 [illegible] at 37 °C with 5% CO_2 in [illegible] for 90 minutes. Image (A): Phase contrast image; Image (B): fluorescent image; Image (C): Merged image of (A) and (B). The scale bar (1 cm) corresponds to [illegible] the 100x objective.

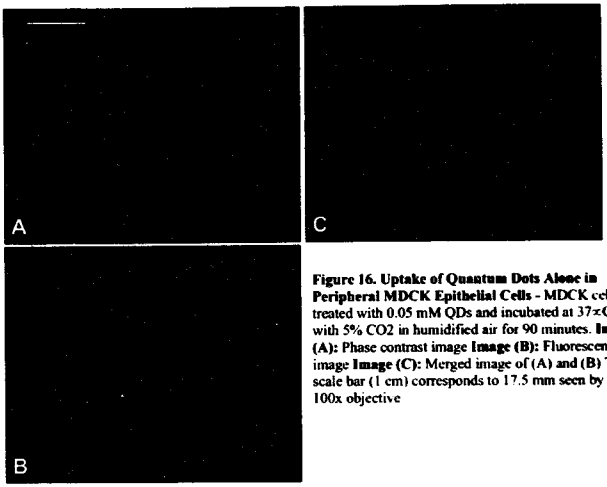

Figure 16. Uptake of Quantum Dots Alone in Peripheral MDCK Epithelial Cells - MDCK cells treated with 0.05 mM QDs and incubated at 37ºC with 5% CO2 in humidified air for 90 minutes. **Image (A):** Phase contrast image **Image (B):** Fluorescent image **Image (C):** Merged image of (A) and (B) The scale bar (1 cm) corresponds to 17.5 mm seen by the 100x objective

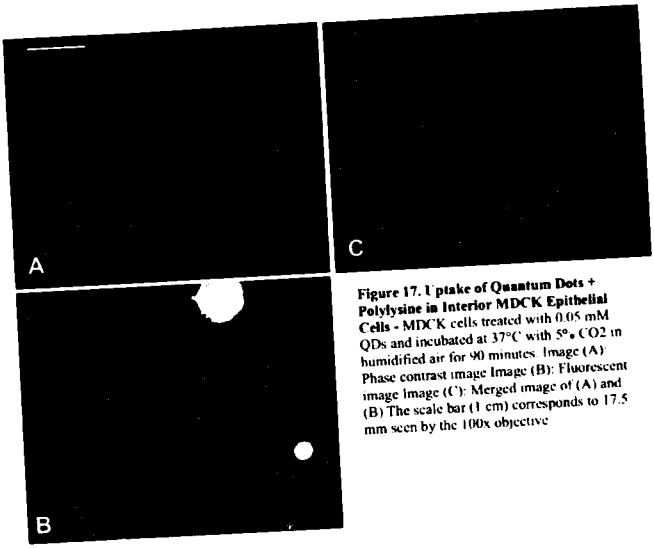

Figure 17. Uptake of Quantum Dots + Polylysine in Interior MDCK Epithelial Cells - MDCK cells treated with 0.05 mM QDs and incubated at 37°C with 5% CO_2 in humidified air for 90 minutes. Image (A) Phase contrast image Image (B): Fluorescent image Image (C): Merged image of (A) and (B) The scale bar (1 cm) corresponds to 17.5 mm seen by the 100x objective

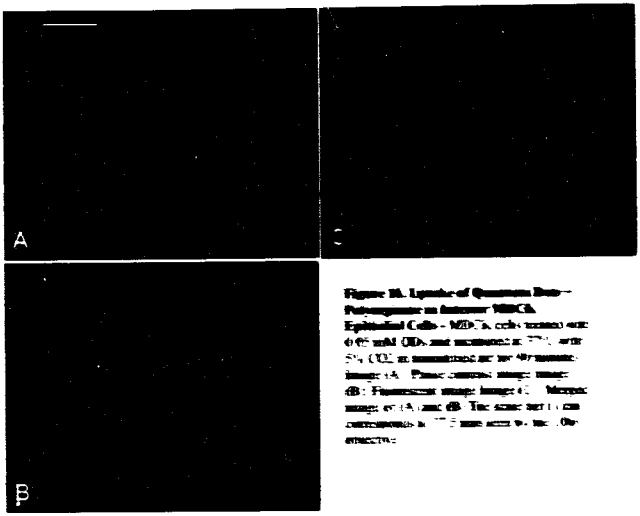

Figure 3A. Uptake of Quantum Dots-Pertuzumab in human MDCK Epithelial Cells - MDCK cells treated with 6 nM QDs and incubated at [illegible] and 5% CO_2 as mentioned in the Materials and Methods section. (A) Phase contrast image. (B) Fluorescence image. (C) Merged image of (A) and (B). The scale bar (1 cm) corresponds to [illegible] as seen in the Objective.